DP-MS-71-31

AN EXPERIMENTAL INVESTIGATION OF THE EFFECTS OF SPACE AND REFLECTION ON THE COUNT-RATE FLUCTUATION SPECTRA OF A LARGE NUCLEAR REACTOR

by

C. O. Thomas, Jr., S. H. Hanauer, and N. P. Baumann

Savannah River Laboratory
E. I. du Pont de Nemours and Co.
Aiken, South Carolina 29801

A Paper for Presentation at the
1971 Winter Meeting of the American Nuclear Society
Miami Beach, Florida
October 17-21, 1971

and

For Publication in
Nuclear Science and Engineering

9/15/71

This document was prepared in conjunction with work accomplished under Contract No. AT(07-2)-1 with the U.S. Department of Energy.

ABSTRACT

Experiments were performed on a large nuclear reactor to investigate the effects of detector placement and reflection on the count-rate fluctuation spectra and the space dependence of the detector efficiency. The magnitudes, break frequencies, and roll-off slopes of the spectra were found to be affected by both detector placement and reflection. The space dependence of the detector efficiency was found to be proportional to that of the average count rates of the detectors.

AN EXPERIMENTAL INVESTIGATION OF THE EFFECTS OF SPACE AND REFLECTION ON THE COUNT-RATE FLUCTUATION SPECTRA OF A LARGE NUCLEAR REACTOR

C. O. Thomas, Jr.*
Savannah River Laboratory
E. I. du Pont de Nemours and Co.
Aiken, South Carolina 29801

S. H. Hanauer**
University of Tennessee
Knoxville, Tennessee 37916

N. P. Baumann
Savannah River Laboratory
E. I. du Pont de Nemours and Co.
Aiken, South Carolina 29801

INTRODUCTION

The use of noise analysis techniques for investigating the dynamic behavior of nuclear reactors as well as inferring certain of their characteristic parameters is well established. One of the most popular methods of reactor noise analysis involves the determination of auto-power-spectral-densities (APSD's) and cross-power-spectral-densities (CPSD's) of count-rate fluctuations from neutron detectors placed in a reactor's neutron field and the interpretation of these spectra in terms of the space-independent reactor model.

* Oak Ridge Graduate Fellow from the University of Tennessee under appointment from the Oak Ridge Associated Universities. Present address: Tennessee Valley Authority.
**Present address: United States Atomic Energy Commission.

Since reactors are actually finite and can be reflected, consideration must be given to any effects that detector placement (space effects) and reflection (reflector effects) can have on the reactors count-rate fluctuation spectra. Although several theoretical models have been developed that predict space and reflector effects, relatively little experimentation has been performed to actually describe these effects. In this study, space and reflector effects, and also the spatial behavior of the correlated-to-uncorrelated ratio (C/U), and thus the spatially-dependent detector efficiency, were determined experimentally, and the results were compared with those predicted by several existing theoretical models.[1]

EXPERIMENTAL DETAILS

The Reactor

The reactor used for this study is Savanah River Laboratory's Process Development Pile (PDP), a large critical facility used for low-power reactor physics studies of heavy-water-moderated lattices.[2] The PDP consists of a cylindrical tank, approximately 494 centimeters in diameter and 488 centimeters high, in which core elements can be suspended. Reactivity is controlled by varying the position of poison rods and the moderator height.

Diagrams of the two lattices used for this study, the poisoned boundary lattice and the reflected boundary lattice, are shown in Figures 1 and 2, respectively. Both lattices contained 19 vertical hexagonal cells arranged to form cylindrical cores approximately 211 centimeters in diameter. Each hexagonal cell consisted of a control rod cluster surrounded by six enriched-uranium fuel assemblies. Both lattices were moderated with heavy water, were reflected at their bottoms by approximately 40 centimeters of heavy water, and were unreflected at their tops. The reflected boundary lattice was reflected radially by approximately 142 centimeters of heavy water. Lithium-aluminum poison rods were placed in the heavy water immediately surrounding the core to produce a nonreflected radial boundary condition for the poisoned boundary lattice.

The calculated neutron migration lengths for both lattices were 13.5 centimeters. The subcriticalities and corresponding effective core heights were 33.3 cents and 233.1 centimeters, respectively, for the poisoned boundary lattice and 31.3 cents and 221.5 centimeters, respectively, for the reflected boundary lattice. Neutrons were provided by the spontaneous fissioning of the fuel and by a small plutonium-beryllium source located above the surface of the water such that the count rates from the detectors in the region of the maximum neutron flux could be accommodated by the instrumentation.

Ten neutron detectors were used in the poisoned boundary lattice and 18 neutron detectors were used in the reflected boundary lattice, as shown in Figures 1 and 2, respectively. The detectors were located in pairs at equivalent hexagonal positions along corresponding diameters of each lattice and were centered vertically on the effective core heights. The neutron detectors are proportional counters filled to a pressure of 152 centimeters of mercury with boron-trifluoride enriched to 96 percent in boron-10. The detectors have active diameters and lengths of 2.5 and 30.5 centimeters, respectively.

Data Acquisition

Data was acquired by recording synchronously on magnetic tape the output signals of identical neutron counting systems connected to selected neutron detectors. Each counting system consisted of a preamplifier, a pulse amplifier-discriminator, a count-rate integrator with a 100-microsecond time constant, and a high-pass filter. A scaler and timer were used to determine average count rates.

For both the poisoned and reflected boundary lattices, data were recorded for cases in which the detectors were located together, for cases in which the detectors were located symmetrically, and for cases in which one detector was always kept at the center of the reactor. For each case, data were recorded for 30 minutes.

Data Reduction

Data was reduced by digitizing selected pairs of the tape-recorded data, computing values of the count-rate fluctuation spectra of each digitized signal pair, correcting the computed spectral values for tape-speedup and frequency and count-rate response of the instrumentation, and fitting simple analytical functions of frequency to the spectral values to determine quantitatively their magnitudes, break frequencies, and roll-off slopes.

Values of the count-rate fluctuation spectra were determined by means of CROSSPOW, a fast-Fourier-transform digital spectral analysis code that calculates values of the APSD's and both the magnitude and phase of the CPSD of a serially-digitized signal pair.[3]

The values of the APSD's were least-squares fitted by the function

$$\mathrm{APSD}(f) = \frac{A}{|1 + jf/B|^{D}} + E \qquad (1)$$

where A, B, and D are fitting parameters that represent, respectively, the low-frequency magnitude, break frequency, and roll-off slope of the correlated component, and E represents the magnitude of the uncorrelated component of the APSD. The values of the magnitudes of the CPSD's were least-squares fitted by the function

$$|\mathrm{CPSD}(f)| = \frac{F}{|1 + jf/G|^{H}} \qquad (2)$$

where F, G, and H are fitting parameters that represent, respectively, the low-frequency magnitude, break frequency, and roll-off slope of the magnitude of the CPSD. The values of the C/U's were inferred from the low-frequency magnitudes of the correlated components and the magnitudes of the uncorrelated components of the APSD's. For the APSD represented by Equation (1), the C/U was determined by $$\frac{C}{U} = \frac{A}{E}$$ (3)

RESULTS

For both the poisoned and reflected boundary lattices, CPSD's were obtained for cases in which the detectors were located together, for cases in which the detectors were located symmetrically, and for cases in which one detector was always located at the center of the reactor. The magnitudes and phases of the CPSD's for the cases in which both detectors were located at the centers of the poisoned and reflected boundary lattices are shown in Figures 3 and 4, respectively. The solid curves in these figures are least-squares fits of Equation (2) to the spectral values.

Equation (2) describes adequately the magnitudes of all the CPSD's except those for cases in the reflected boundary lattice in which both detectors were located together just inside the reflector, and both detectors were located on opposite sides of the reactor just inside the reflector. These spectra, shown in Figures 5 and 6, respectively, exhibit anomalous dips or peaks at frequencies near their break frequencies. Buhl observed this phenomenon in Savannah River Laboratory's 305 Test Pile.[4]

The values of the low-frequency magnitudes, break frequencies, and roll-off slopes of the magnitudes of the CPSD's are shown in Figures 7, 8, and 9, respectively. From these figures, it can be seen that the low-frequency magnitudes, break frequencies, and roll-off slopes of the magnitudes of the CPSD's are affected by both detector placement and reflection. Also, the values of the break frequencies of the CPSD's for reflected boundary lattice are significantly less than those of the poisoned boundary lattice. This difference is attributed to the significantly greater prompt neutron lifetime of the reflected boundary lattice.

The phases of the CPSD's were nearly zero for the cases in which the detectors were located together or symmetrically. For the cases in which one detector was always located at the center of the reactor, the responses of the off-axis detectors lagged that of the central detector at the higher frequencies. This lag is illustrated in Figure 10 which shows the magnitude and phase of the CPSD for the case in which one detector was located at the center of the reactor and the other detector was located just inside the reflector of the reflected boundary lattice.

The magnitudes of the CPSD's predicted for the critical reflected boundary PDP predicted by the space independent reactor model and by Cohn's two-node reflected reactor model[5] are shown in Figure 11. The low-frequency magnitudes of these curves were normalized to unity to show more clearly the differences in their break frequencies and roll-off slopes. The magnitudes of the CPSD's predicted by the space-independent reactor model were determined for both the effective and core-averaged prompt neutron lifetimes which were 714 and 231 microseconds, respectively. The difference in the values of the break frequencies of these two curves is due entirely to the difference in the prompt neutron lifetimes. The values of the roll-off slopes of both of these curves is 2.0 decades/decade.

The magnitudes of the CPSD's predicted by Cohn's two-node reflected reactor model were determined for the case in which both detectors are located in the reflector and for the case in which both detectors are located in the core. The two curves are almost identical for frequencies below two Hertz. However, the value of the roll-off slope of the magnitude of the CPSD for the case in which both detectors are located in the reflector is significantly greater than the value of 2.0 decades/decade predicted by the space-independent reactor model, and the magnitude of the CPSD for the case in which both detectors are located in the core appears to be influenced by an extra pole and zero at approximately 15 Hertz. Cohn predicted that the extra pole and zero should not affect the magnitude of the CPSD in the frequency range accessible to present-day noise analysis techniques for reactors in which the prompt neutron lifetimes of the core and reflector are of the same order of magnitude; however, the prompt neutron lifetime of the heavy-water reflector of the PDP, approximately 19 milliseconds, is over 25 times greater than the effective prompt neutron lifetime of the core.

Although the deviation from a constant roll-off slope is not as great as that predicted by Cohn's model, the magnitude of the CPSD for detectors located at the center of the reflected boundary lattice shown in Figure 4 does appear to be influenced by an extra pole and zero at about 25 Hertz. Equation (2) was least-squares fitted to the values of the magnitudes of the CPSD's predicted by Cohn's model to determine quantitatively their roll-off slopes. The roll-off slope of the magnitude of the CPSD for the case in which both detectors are located in the reflector is 2.1 decades/decade and that for the case in which both detectors are located in the core is 1.5 decades/decade. The roll-off slopes determined from the least-squares fitted values of the magnitudes of the CPSD's for the detectors at the center and for detectors just inside the reflector in the reflected boundary lattice are 1.2 and 2.9 decades/decade, respectively. Therefore, although the values of the spectral parameters of the magnitudes of the CPSD's calculated by Cohn's model do not agree exactly with those determined experimentally, the model does predict qualitatively the general features observed in the experimentally-determined magnitudes of the CPSD's for the reflected boundary lattice.

The values of the C/U's, which were inferred from the least-squares fitted low-frequency magnitudes of the correlated components and the magnitudes of the uncorrelated components of the APSD's, are shown as functions of distance from the reactor center for the poisoned boundary and reflected boundary lattices in Figures 12 and 13, respectively, where these values are represented by open circles. The experimentally-determined average count rates of the detectors, normalized to the values of the C/U's at the center of the reactors, are represented by open squares in Figures 12 and 13.

In addition, values of the average count rates of the detectors were calculated by the two-dimensional, four-energy-group reactor diffusion code PDQ-5[6] using four-energy-group cell-averaged parameters calculated by HAMMER.[7] These values, normalized to the values of the C/U's at the centers of the reactors, are represented by open triangles in Figures 12 and 13.

Congdon and Albrecht predicted that the space dependence of the detector efficiency is described by that of the adjoint-flux-weighted count rates of the detectors.[8] Values of the adjoint-flux-weighted count rates of the detectors calculated by PDQ-5 and normalized to the values of the C/U's at the centers of the reactors, are represented by darkened squares in Figures 12 and 13. Also included in these figures are values of the product of the macroscopic absorption cross section of the detectors and the adjoint neutron flux, represented by darkened circles, and values of the product of the macroscopic absorption cross section of the detectors and the square root of the product of the neutron flux and its adjoint, represented by darkened triangles. These values were also calculated by PDQ-5 and were normalized to the values of the C/U's at the centers of the reactors.

The space dependence of the C/U's for the poisoned boundary lattice is described adequately by all the functions except the calculated adjoint-flux-weighted count rates. For the reflected boundary lattice, where the space dependence of the neutron flux differs from that of its adjoint considerably more than in the poisoned boundary lattice, the space dependence of the C/U's is described best by that of the experimentally determined average count rates. Of the functions calculated by PDQ-5, the space dependence of the average count rates is the closest to and the space dependence of the adjoint-flux-weighted count rates is farthest from that of the C/U's. That the latter is true is evidenced by the significantly different values of the calculated adjoint-flux-weighted count rates and the experimentally determined values of the C/U's in the reflector region as seen in Figure 13.

CONCLUSIONS

The conclusions reached as a result of this study are as follows:

- The low-frequency magnitudes, break frequencies, and roll-off slopes of the magnitudes of the CPSD's are affected by both detector placement and reflection.
- The CPSD's for the reflected boundary lattices for the cases in which both detectors were located together just inside the reflector, and both detectors were located on opposite sides of the reactor just inside the reflector exhibit anomalous dips or peaks at frequencies near their break frequencies.
- The space dependence of the low-frequency portions of the CPSD's is proportional to that of the product of the average count rates of the detectors.

- The values of the break frequencies of the CPSD's for the reflected boundary lattice are significantly less than those of the poisoned boundary lattice.
- The phases of the CPSD's are nearly zero for the cases in which the detectors were located together or symmetrically. For the cases in which one detector was always located at the center of the reactor, the responses of the off-axis detectors lagged that of the central detector at the higher frequencies.
- Calculations with Cohn's two-node reflected reactor model show qualitatively the general features observed in the experimentally determined CPSD's with both detectors located at the center of the reflected boundary lattice.
- The space dependence of the C/U is proportional to that of the product of average count rates of the detectors. For the reflected boundary lattice, the space dependence of C/U differs significantly from that of the adjoint-flux-weighted average count rates of the detectors calculated with the PDQ-5. Thus, the experimentally-determined detector efficiency was found to be proportional to the neutron flux and not to the adjoint-weighted flux, as predicted by Congdon and Albrecht.

ACKNOWLEDGMENTS

The authors gratefully acknowledge the contributions of Dr. R. C. Kryter of the Instrumentation and Controls Division at Oak Ridge National Laboratory in making available his digital spectral analysis code CROSSPOW; Mr. J. R. Penland of the University of Tennessee in making available his least-squares data fitting code PSDFIT; the Instrumentation and Controls Division of Oak Ridge National Laboratory in making available their Fast Magnetic Tape Data System; and the Nuclear Engineering Department of the University of Tennessee in funding the use of the computer at Oak Ridge National Laboratory for data analysis.

The information contained in this paper was developed during the course of work under Contract AT(07-2)-1 with the United States Atomic Energy Commission.

REFERENCES

1. C. O. Thomas, Jr., "An Experimental Investigation of the Effects of Space and Reflection on the Count-Rate Fluctuation Spectra of a Large Nuclear Reactor," Unpublished Doctoral Dissertation, The University of Tennessee, Knoxville (1971).

2. A. E. Dunklee, "The Heavy Water System of the Process Development Pile," DP-567, Savannah River Laboratory (1967).

3. R. C. Kryter, "Application of the Fast Fourier Transform Algorithm to On-Line Reactor Diagnosis," *IEEE Transactions on Nuclear Science*, Volume NS-16, Number 1, Pages 210-217, February 1969.

4. A. R. Buhl, S. H. Hanauer, and N. P. Baumann, "An Experimental Investigation of Spatial Effects on the Neutron Fluctuation Spectra of a Large Reactor," *Nuclear Science and Engineering*, *34*, 98 (1968).

5. C. E. Cohn, "Reflected-Reactor Kinetics," *Nuclear Science and Engineering*, *13*, 12 (1962).

6. W. R. Cadwell, P. F. Buerger, and C. J. Pfeifer, "The PDQ-5 and PDQ-6 Programs for the Solution of the Two-Dimensional Neutron Diffusion-Depletion Problem," WAPD-TM-477, Westinghouse Atomic Power Division (1965).

7. J. E. Suich and H. C. Honeck, "The HAMMER System," DP-1064, Savannah River Laboratory (1967).

8. M. E. Congdon and R. W. Albrecht, "An Adjoint-Weighting in Neutron Fluctuation Analysis with Emphasis on an Effective Detector Efficiency," *Nuclear Science and Engineering*, *39*, 207 (1970).

PW/bch

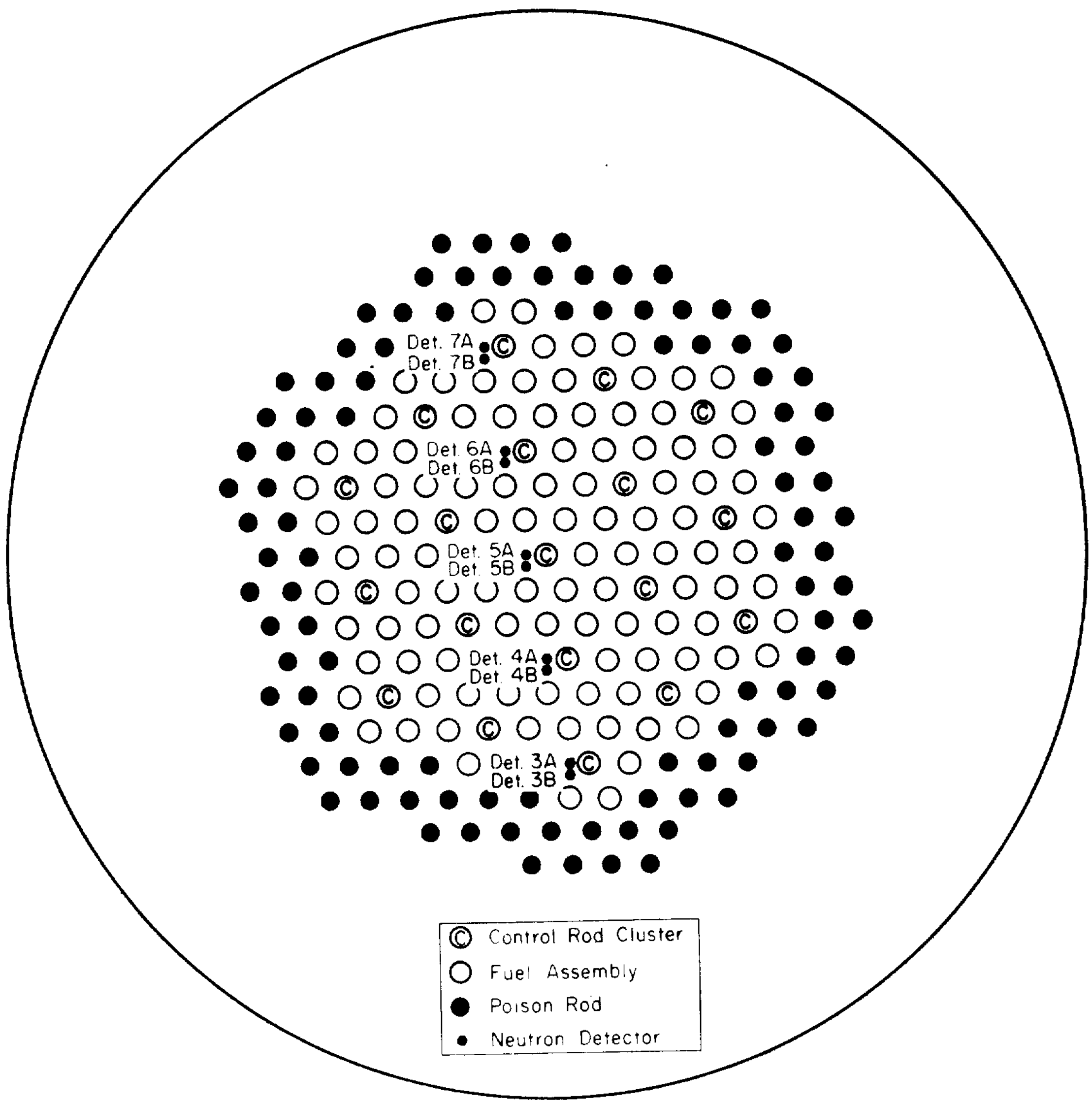

FIG. 1 DIAGRAM OF THE POISONED BOUNDARY PDP LATTICE

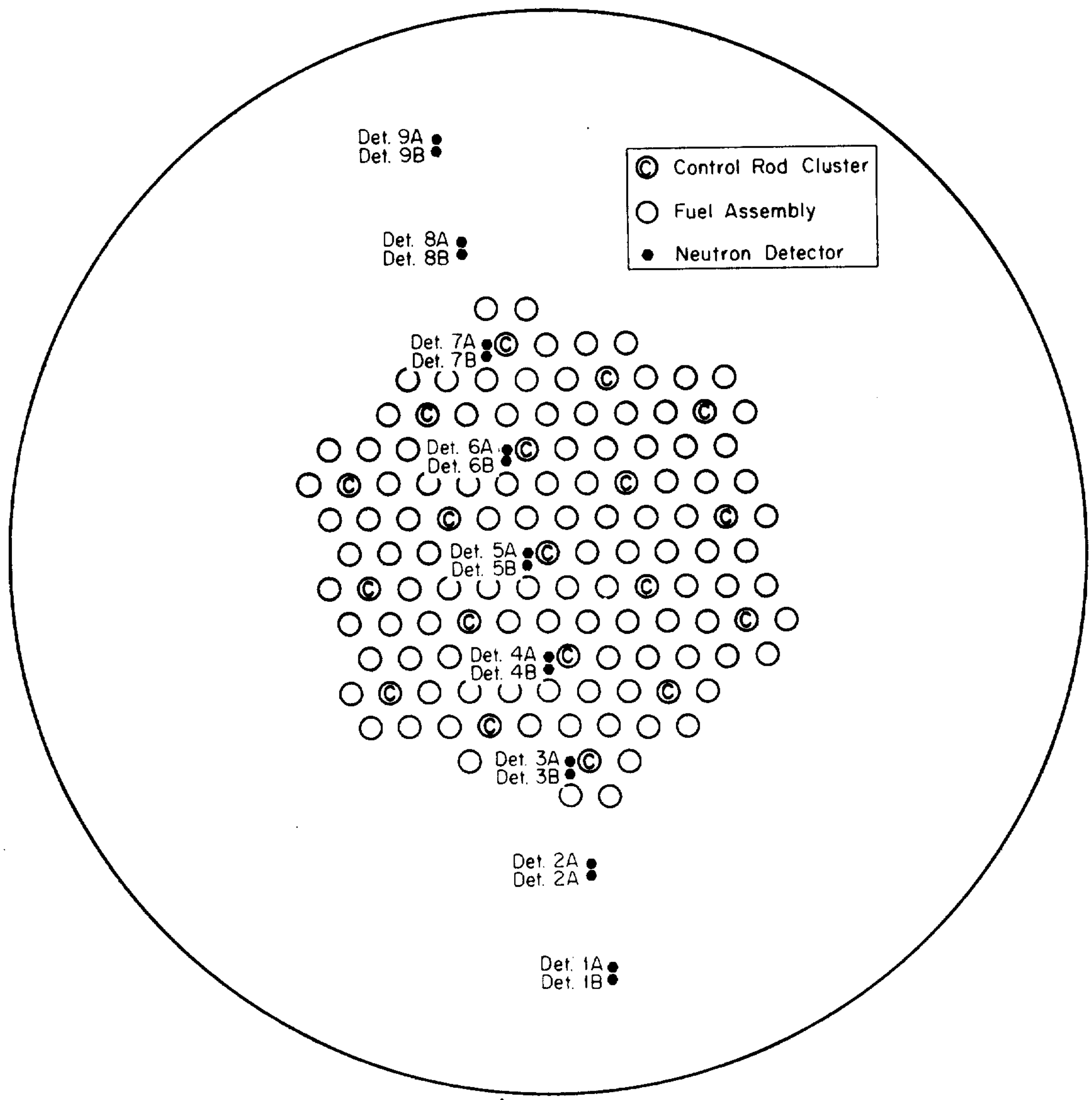

FIG. 2 DIAGRAM OF THE REFLECTED BOUNDARY PDP LATTICE

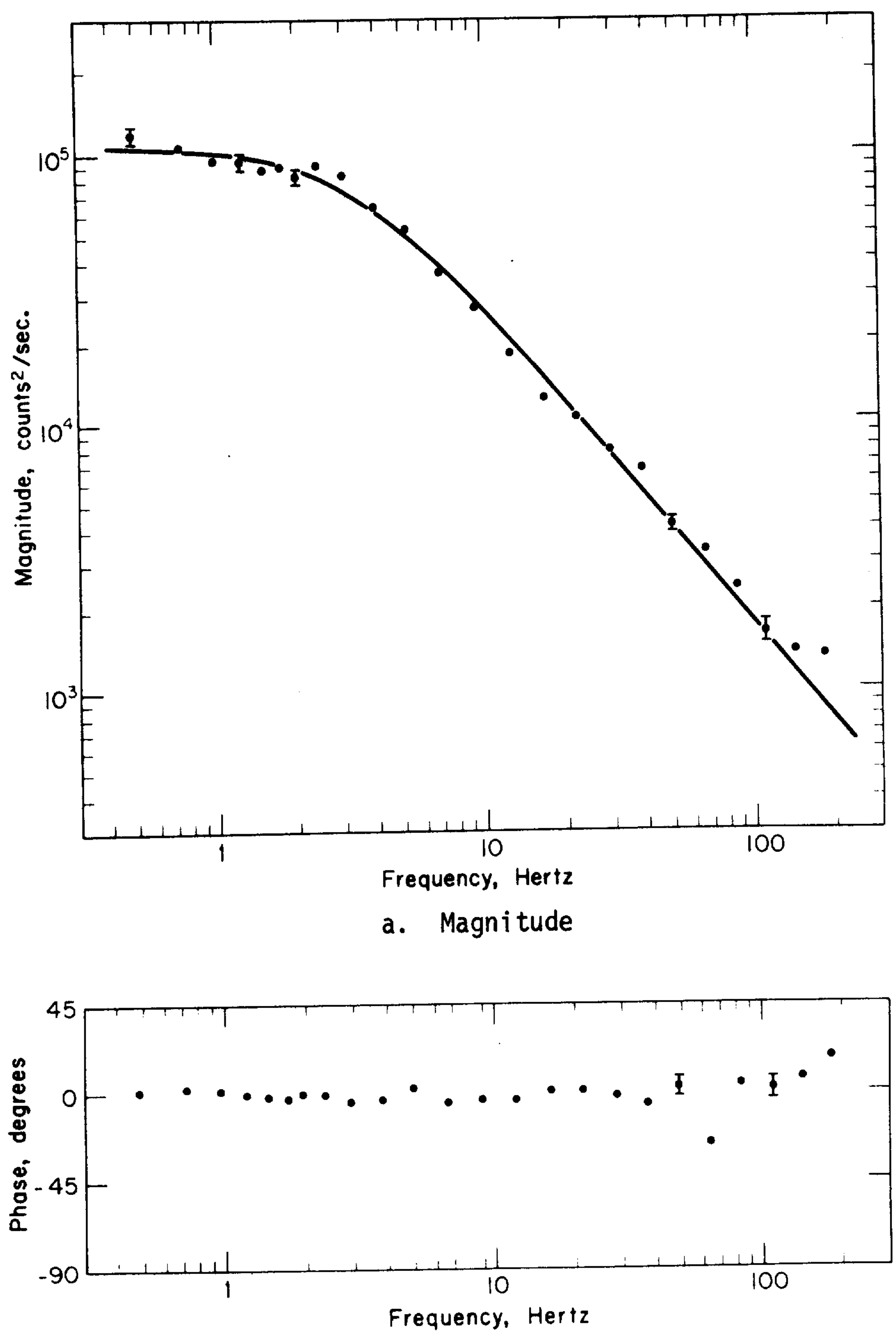

a. Magnitude

b. Phase

FIG. 3 MAGNITUDE AND PHASE OF THE CPSD FOR DETECTORS LOCATED AT THE CENTER OF THE POISONED BOUNDARY PDP

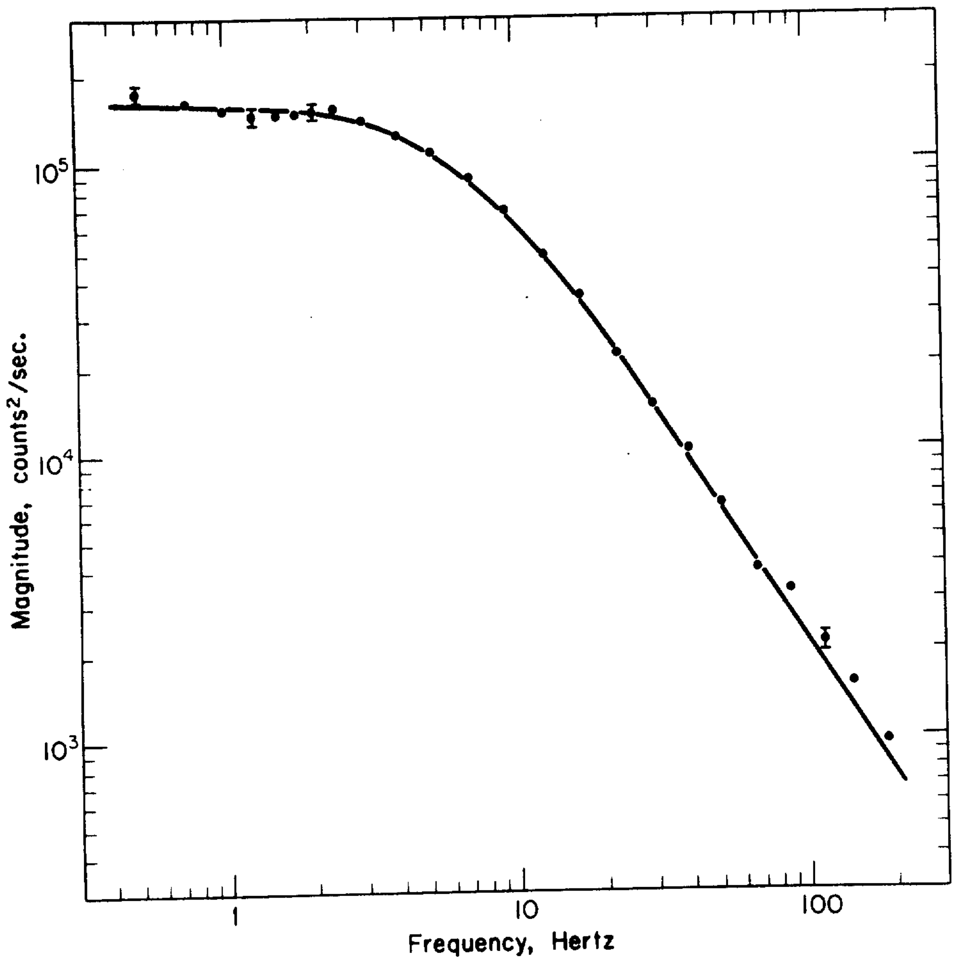

a. Magnitude

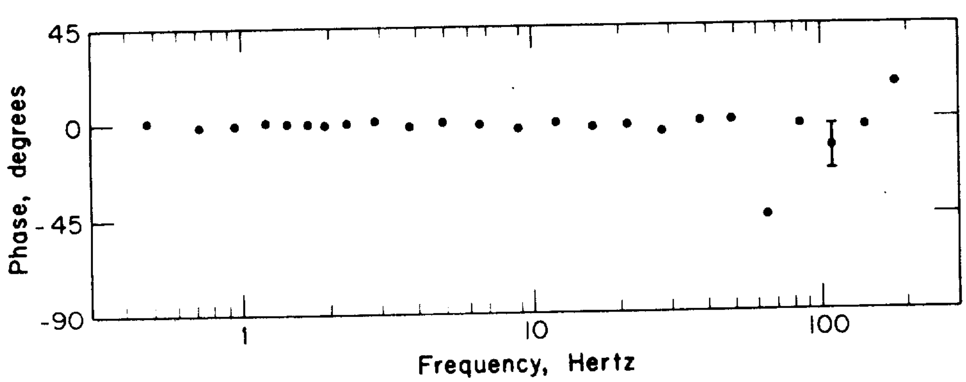

b. Phase

FIG. 4 MAGNITUDE AND PHASE OF THE CPSD FOR DETECTORS LOCATED AT THE CENTER OF THE REFLECTED BOUNDARY PDP

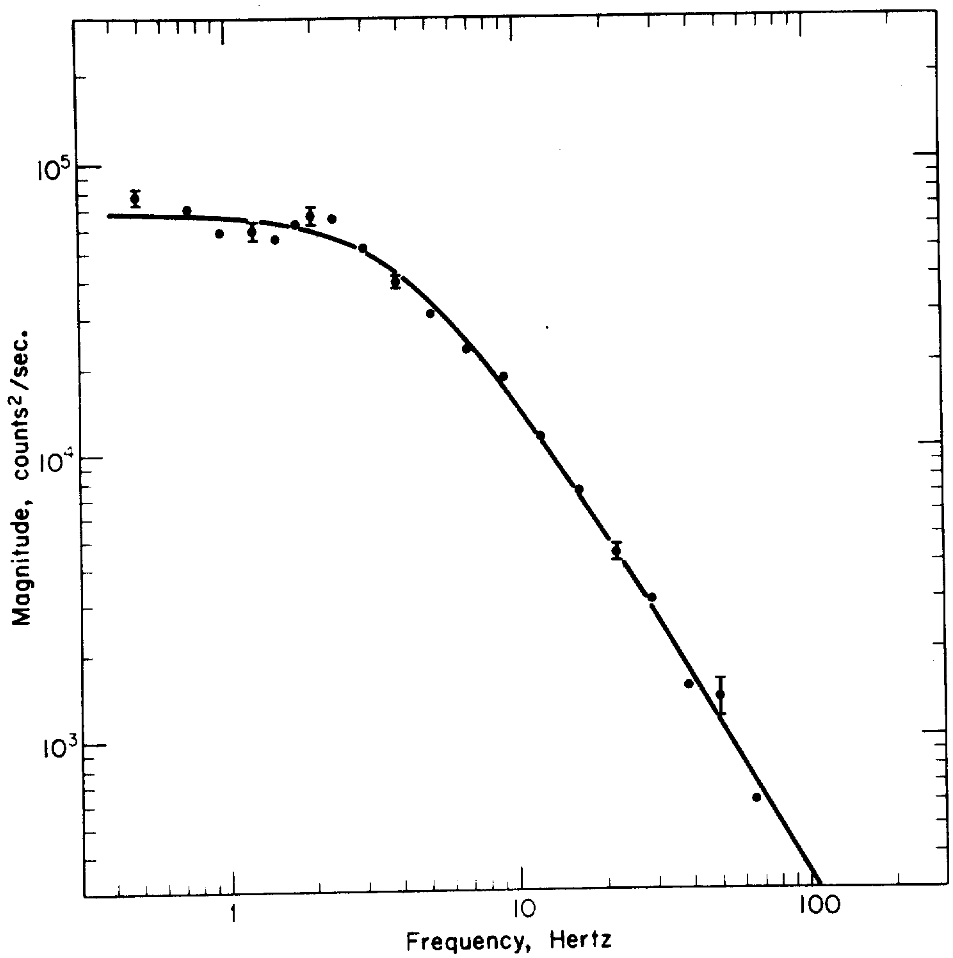

a. Magnitude

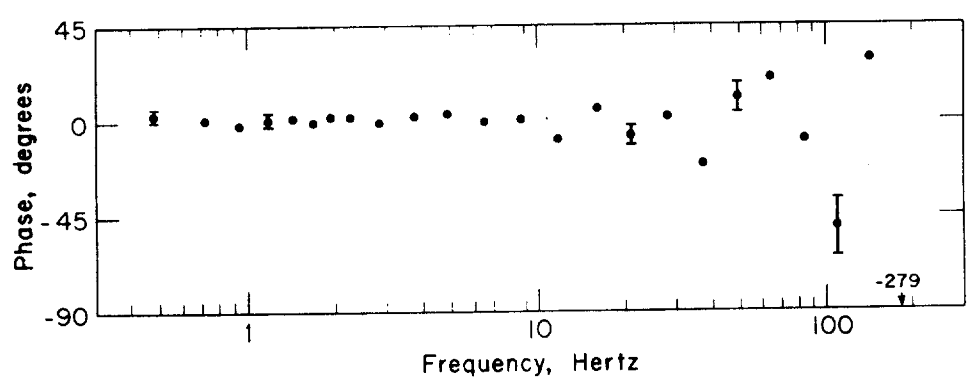

b. Phase

FIG. 5 MAGNITUDE AND PHASE OF THE CPSD FOR DETECTORS LOCATED TOGETHER JUST INSIDE THE REFLECTOR OF THE REFLECTED BOUNDARY PDP

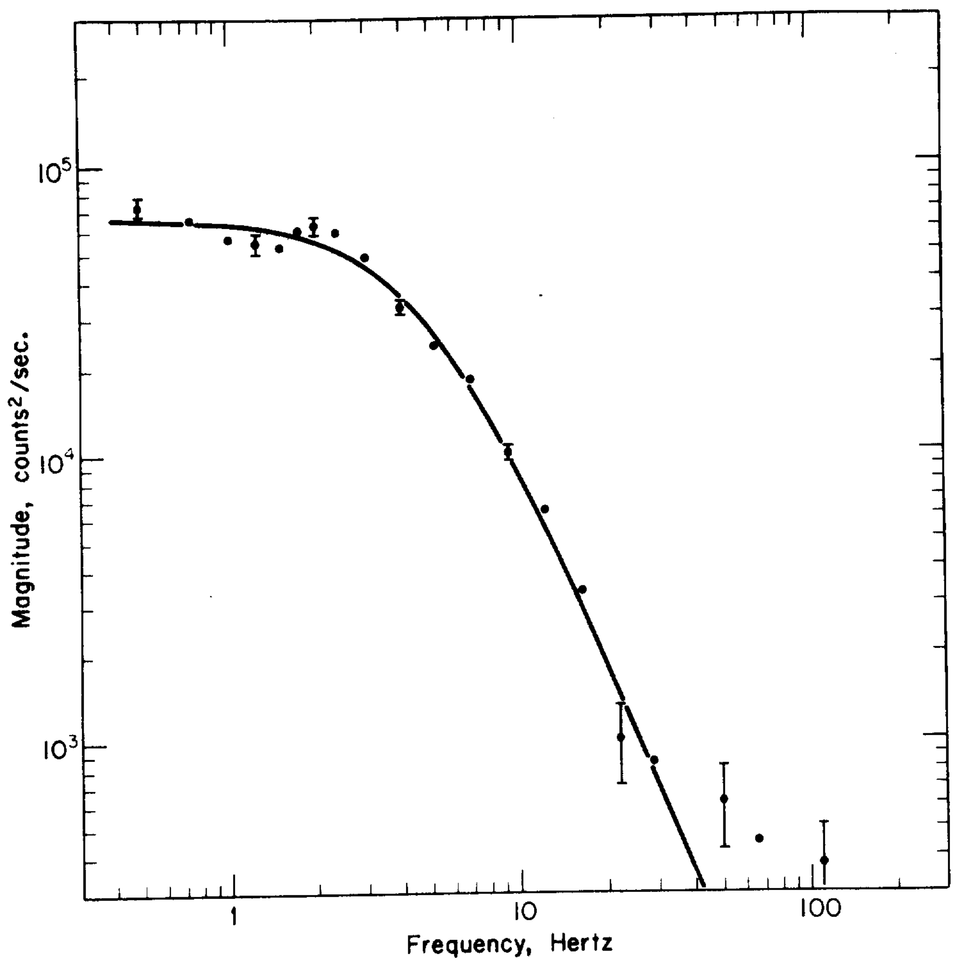

a. Magnitude

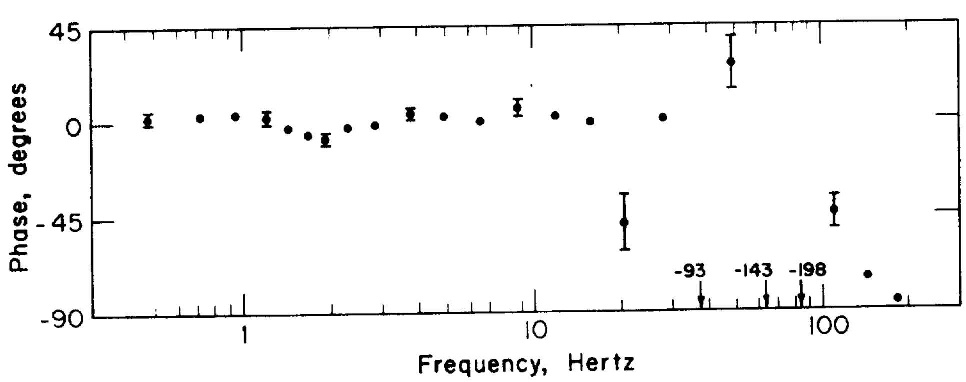

b. Phase

FIG. 6 MAGNITUDE AND PHASE OF THE CPSD FOR DETECTORS LOCATED ON OPPOSITE SIDES OF THE REACTOR JUST INSIDE THE REFLECTOR OF THE REFLECTED BOUNDARY PDP

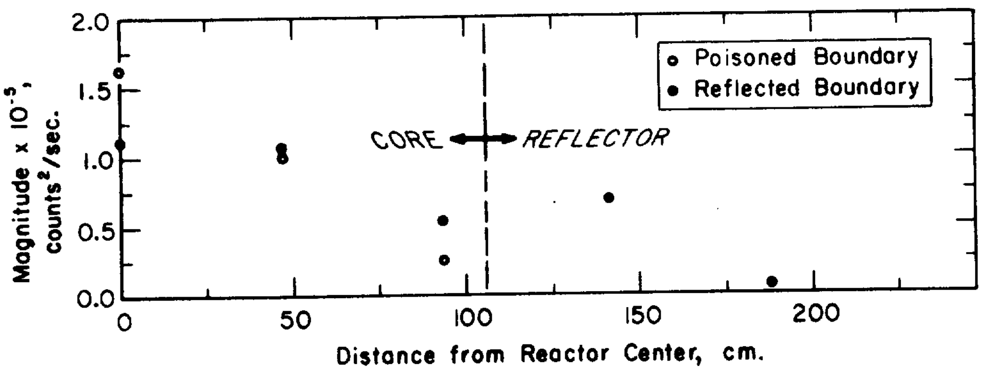

a. Detector located together

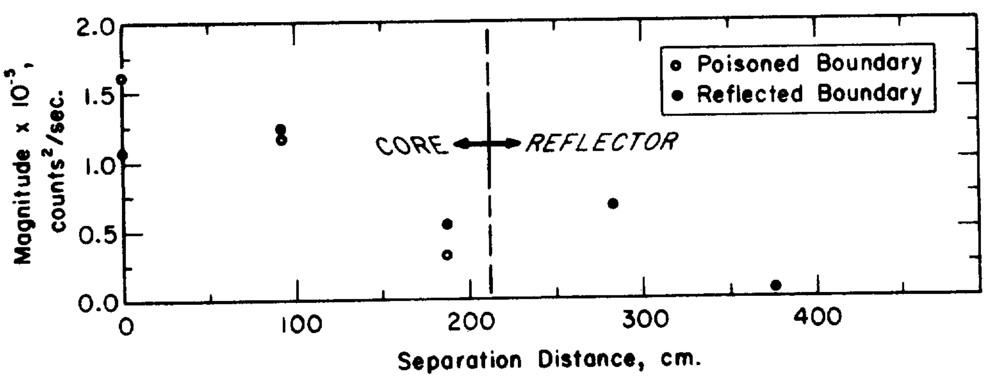

b. Detectors located symmetrically

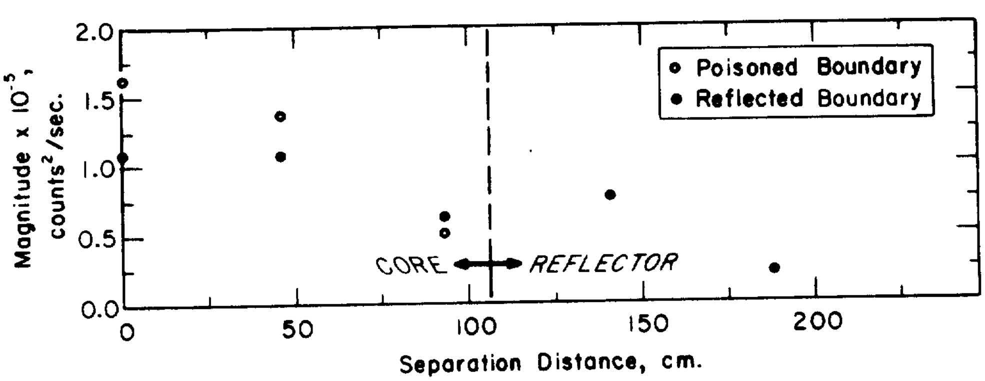

c. One detector located at the reactor center

FIG. 7 COMPARISON OF THE LOW-FREQUENCY MAGNITUDES OF THE MAGNITUDES OF THE CPSD'S FOR THE PDP RUNS

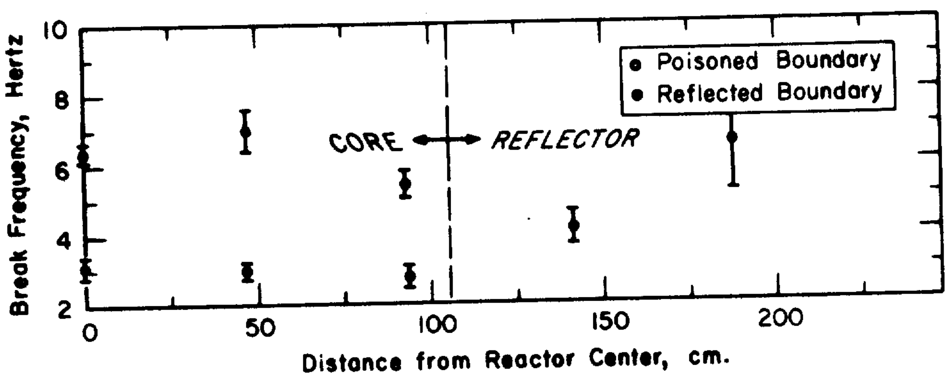

a. Detector located together

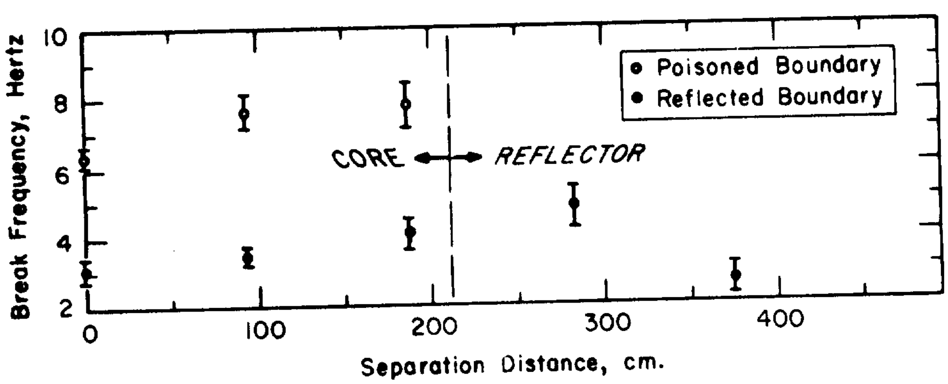

b. Detectors located symmetrically

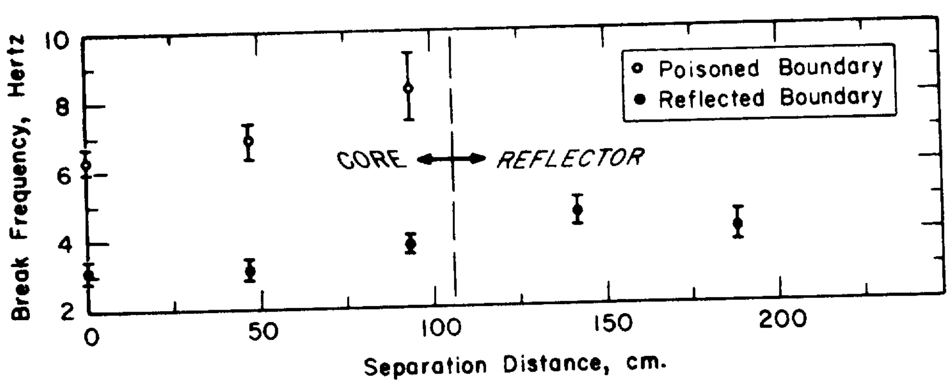

c. One detector located at the reactor center

FIG. 8 COMPARISON OF THE BREAK FREQUENCIES OF THE MAGNITUDES OF THE CPSD'S FOR THE PDP RUNS

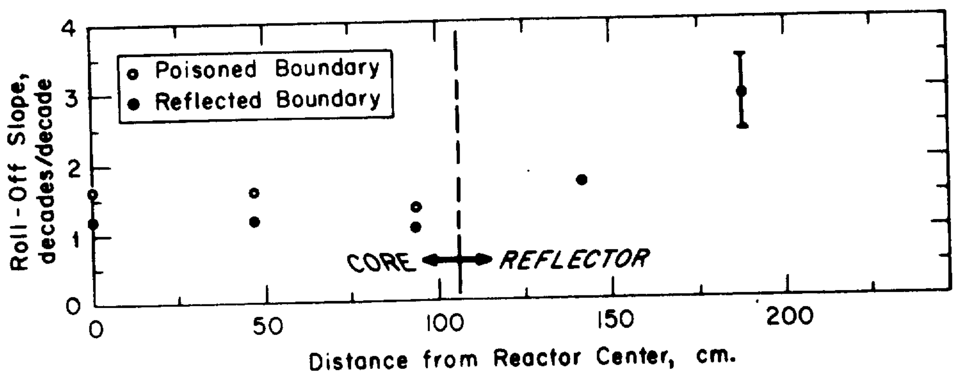

a. Detector located together

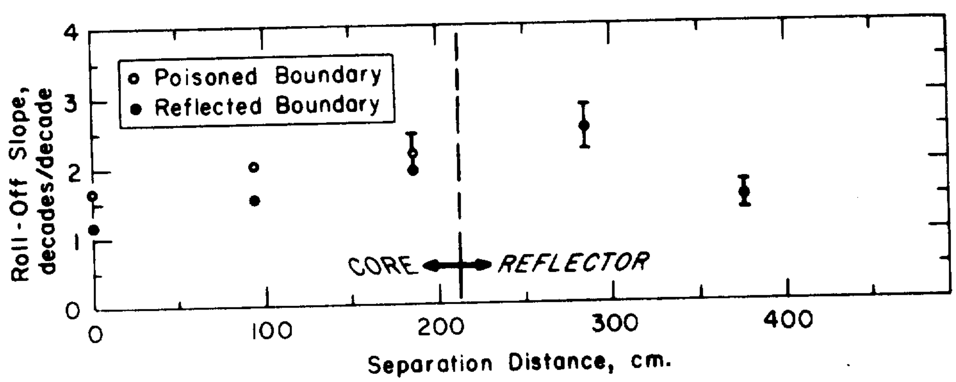

b. Detectors located symmetrically

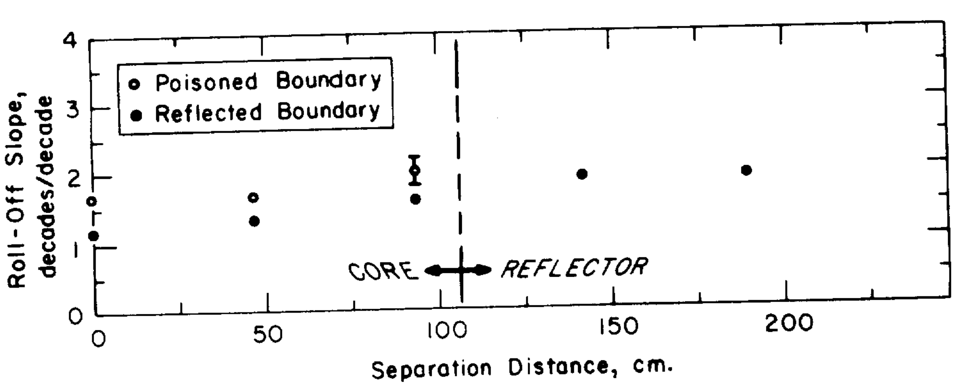

c. One detector located at the reactor center

FIG. 9 COMPARISON OF THE ROLL-OFF SLOPES OF THE MAGNITUDES OF THE CPSD'S FOR THE PDP RUNS

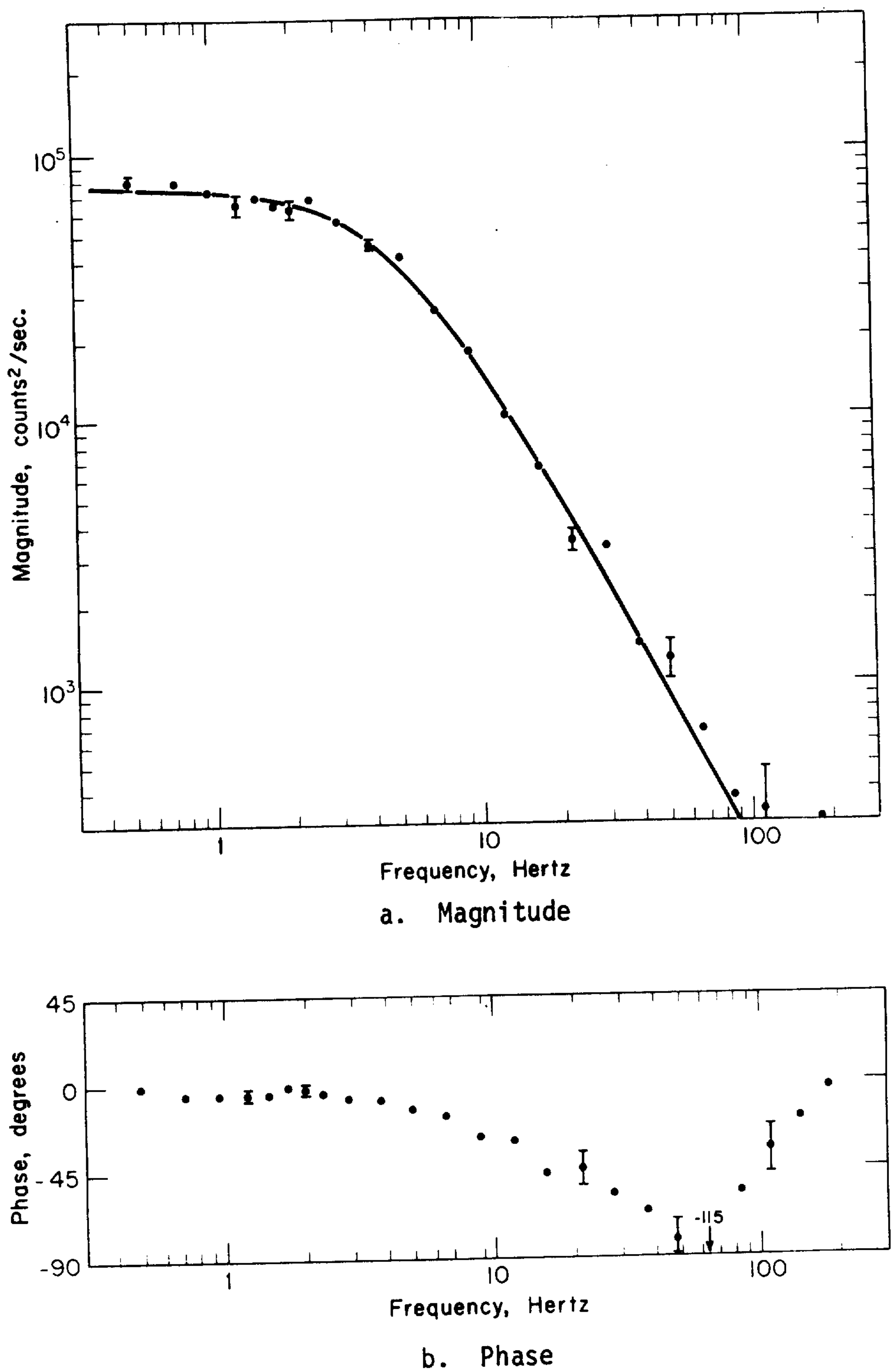

FIG. 10 MAGNITUDE AND PHASE OF THE CPSD FOR ONE DETECTOR LOCATED AT THE CENTER OF THE REACTOR AND THE OTHER DETECTOR LOCATED JUST INSIDE THE REFLECTOR OF THE REFLECTED BOUNDARY PDP

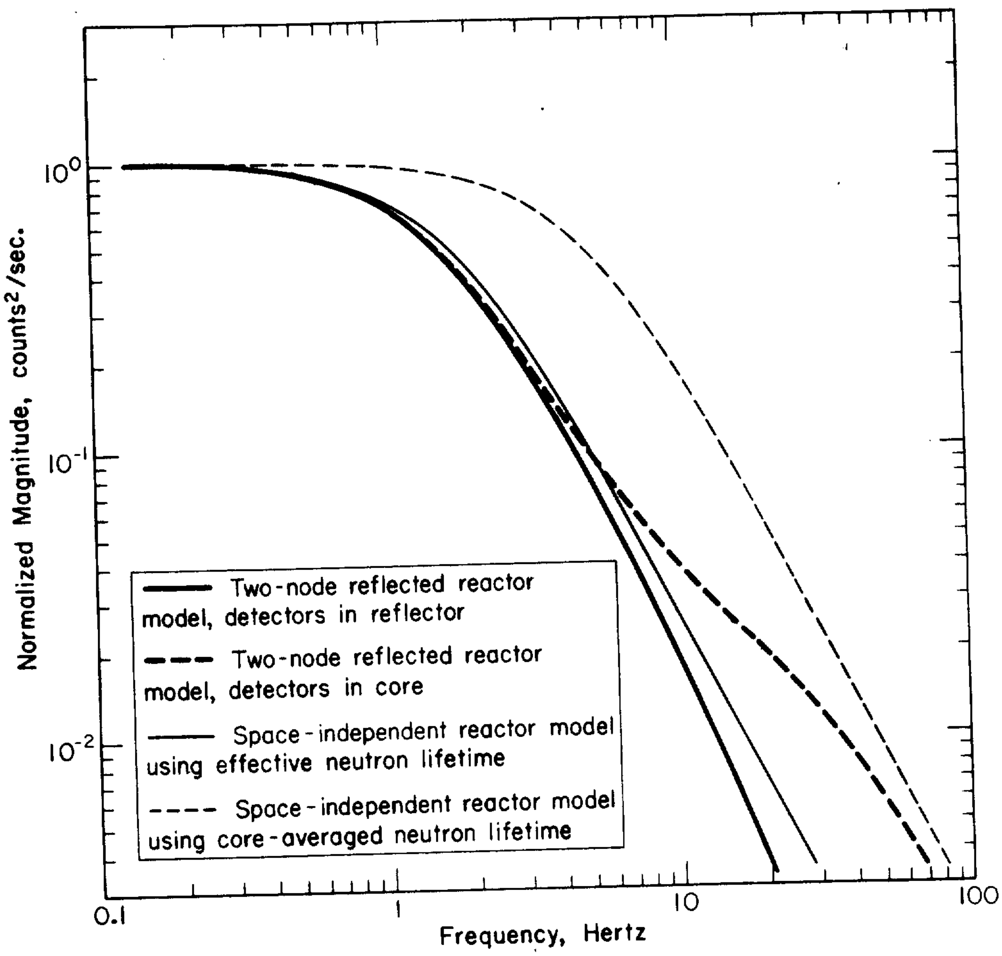

FIG. 11 THEORETICAL MAGNITUDES OF THE CPSD'S FOR THE CRITICAL REFLECTED BOUNDARY PDP

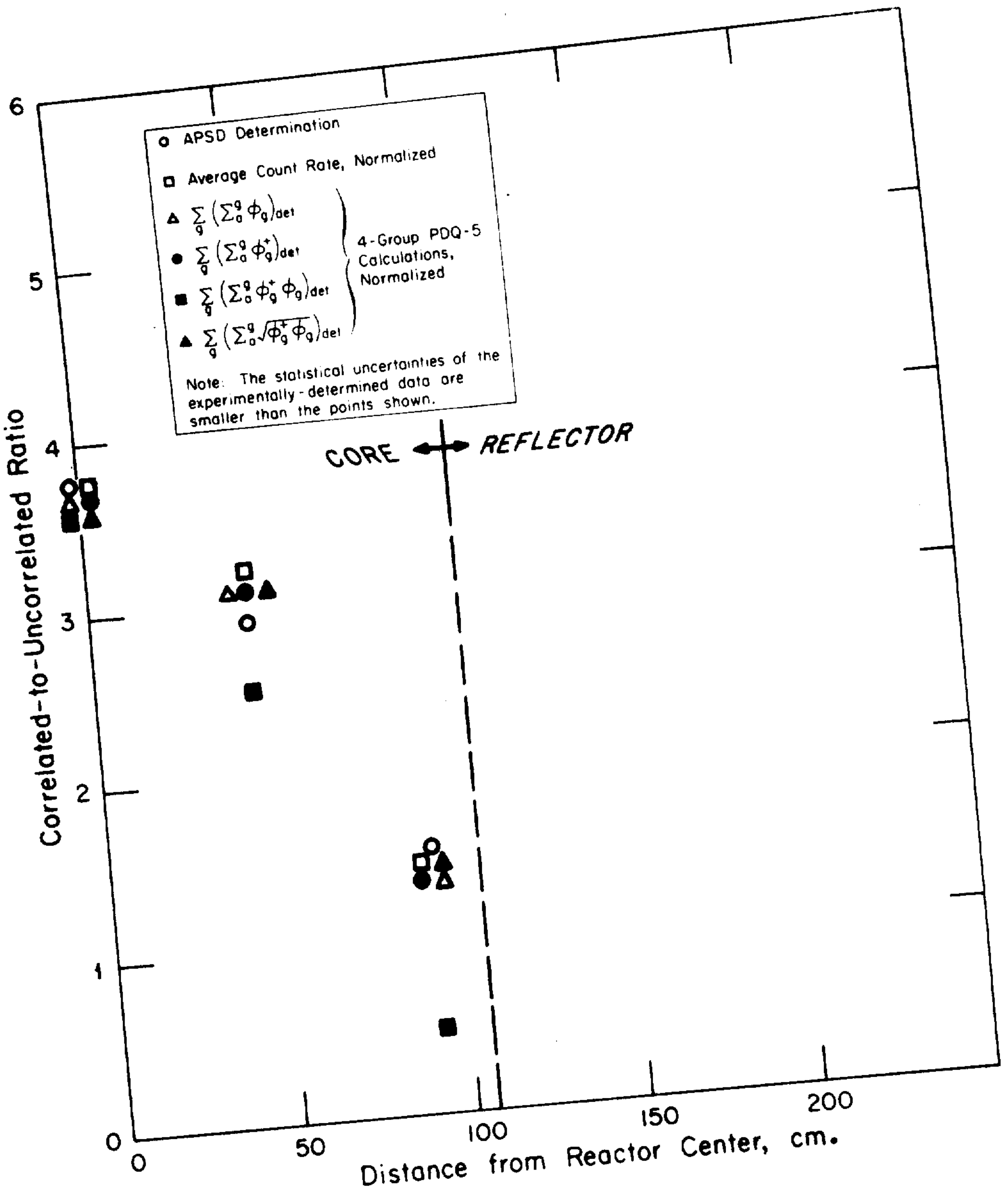

FIG. 12 COMPARISON OF THE CORRELATED-TO-UNCORRELATED RATIOS FOR THE POISONED BOUNDARY PDP